Volume 19, No 1 | International Journal of Radiation Research, January 2021

Comprehensive end-to-end test for intensity-modulated radiation therapy for nasopharyngeal carcinoma using an anthropomorphic phantom and EBT3 film

J. Bao[1,3], L. Chen[2*], J.H. Zhu[2], Z.F. Fei[3,4], Z.T. Hu[3], H.Z. Wang[1,3], Y. Gao[1]

[1]Anhui Province Key Laboratory of Medical Physics and Technology, Institute of Health and Medical Technology, Hefei Institutes of Physical Science, Chinese Academy of Sciences, Hefei, Anhui, China
[2]Department of Radiation Oncology, Sun Yat-Sen University Cancer Center, State Key Laboratory of Oncology in South China, Collaborative Innovation Center for Cancer Medicine, Guangdong Key Laboratory of Nasopharyngeal Carcinoma Diagnosis and Therapy, Guangzhou, Guangdong, China
[3]Department of Radiation Oncology, Hefei Cancer Hospital, Chinese Academy of Sciences, Hefei, Anhui, China
[4]Department of Radiation Oncology, The Joint Logistics Support Force NO.901 Hospital, Hefei, Anhui, China

[DOR: 20.1001.1.23223243.2021.19.1.4.5]
[DOI: 10.29252/ijrr.19.1.31]

► ***Original article***

***Corresponding authors:**
Li Chen, M.D.,
E-mail:
chenli@sysucc.org.cn

Revised: January 2020
Accepted: January 2020

Int. J. Radiat. Res., January 2021; 19(1): 31-39

DOI: 10.29252/ijrr.19.1.31

ABSTRACT

Background: In head and neck radiotherapy, immobilization devices can affect dose delivery. In this study, a comprehensive end-to-end test was developed to evaluate the accuracy of radiotherapy treatment. ***Materials and Methods*:** An Alderson Radiation Therapy (ART) anthropomorphic phantom with EBT3 film was used to mimic the actual patient treatment process. Ten patients treated for nasopharyngeal carcinomas with IMRT were retrospectively selected. For each patient, the treatment plan, as well as the targets and OARs was transplanted onto the phantom, and the IMRT plan was subsequently recalculated to the phantom with EBT3 film. Two quality assurance (QA) plans were generated, namely "Plan-with" wherein the immobilization device was contoured and "Plan-without" wherein it was omitted. EBT3 measurements were compared with the results of the TPS calculation. ***Results:*** With different gamma calculation criteria applied, the results obtained for Plan-with were closer to the dose measured with the EBT3 film. Moreover, 1.8% deviation was observed in the posterior neck skin dose for Plan-with when compared to the film measurements while the value was 33.1% lower for Plan-without. When compared to Plan-without, each target volume in Plan-with exhibited a 1–4% reduction in the maximum dose ($D_{2\%}$), minimum dose ($D_{98\%}$) and mean dose (D_{mean}). ***Conclusion:*** Immobilization devices decrease the radiation dose to target volumes while increasing the skin dose and should be included within the body contour to ensure an accurate planning dose. The end-to-end IMRT test using an ART anthropomorphic phantom is a valuable tool to identify discrepancies between calculated and delivered radiation doses.

Keywords: *End-to-end test, anthropomorphic phantom, EBT3 film; nasopharyngeal carcinoma, intensity-modulated radiation therapy.*

INTRODUCTION

Intensity-modulated radiation therapy (IMRT) is one of the main radiation-therapy techniques that are used to treat nasopharyngeal carcinomas (NPC) [1-3]. To ensure the accuracy and repeatability of the position setting in each radiation therapy

session, some immobilization devices (for e.g., thermoplastic films and vacuum bags) are typically used in clinical practice. Studies have implicated that the materials used to fabricate the treatment table and immobilization device are not air equivalent, and thus radiation beam propagation is affected by the aforementioned devices. For example, the treatment table exhibits a significant attenuating effect on incident radiation [4, 5].

A key component of patient-specific quality assurance (QA) corresponds to ensuring that the dose received by the patient is consistent with the dose planned in the TPS. Currently available radiation-therapy plan verification equipment, such as ionization chambers and plane-detection equipment, significantly differ from actual patient geometry (for e.g., in their shape and density), and the effect of the patient's immobilization device on the dosimetry of the plan delivery is typically not considered during plan verification. It were recommended in the American Association of Physicists in Medicine working group reports Nos. 176 and 218 that the effects of treatment accessories on dose be taken into account in the clinical practice of radiation therapy planning [6], and that plan verification should better approximate actual plan delivery [7].

The end-to-end test verifies the entire treatment process from CT simulation to the end of treatment delivery. It is advantageous over other QA methods which test each parameter individually. The results of an end-to-end test can also ensure confidence in the ability to calculate the delivered dose [8]. Therefore, this type of testing is also recommended after treatment planning system commissioning by AAPM TG-40 and after treatment planning system changes by AAPM TG-142, and TG-53 [9-11]. Most extant studies on the end-to-end test are based on considerably simple phantoms [12-16]. Recently, anthropomorphic phantoms that realistically simulate anatomically accurate patient tissue heterogeneities were introduced to end-to-end IMRT/VMAT dosimetry audit methodology and monthly QA protocol for external beam radiation therapy treatment [17, 18]. To the best of the authors' knowledge, previous studies did not consider the effect of immobilization devices.

In the present study, an Alderson Radiation Therapy (ART) inhomogeneous anthropomorphic head phantom was used to simulate the shape and density, as well as other relevant information of actual patients with NPC. Additionally, an end-to-end test for head and neck IMRT treatments was performed by considering the effect of immobilization devices. We compared the dose distribution calculated by TPS with the delivered dose as measured by EBT3 film. The results were subsequently analyzed to evaluate the delivered dose accuracy of IMRT plans for NPC.

MATERIALS AND METHODS

ART phantom and immobilization

The ART phantom used in the experiments is transected horizontally into 2.5-cm slices and is shown in figure 1. Each slice is designed to contain holes at specific locations that are plugged with bone-tissue-equivalent, soft-tissue-equivalent, or lung-tissue-equivalent materials to mimic the real human anatomy. To simulate a real patient treatment scenario, the ART phantom was placed within a head-and-neck immobilization device (ID) system that was used for patient localization during the IMRT treatment planning and delivery process in the department. The simulation process was performed in the supine position. The head-and-neck immobilization device (ID) system included a carbon fiber base plate, Styrofoam bag, and thermoplastic film placed on the phantom.

Image acquisition and ROI delineation

A CT simulator (Brilliance, Philips Medical Systems, Amsterdam, Netherlands) was used to obtain patient and phantom images, and to scan the phantom over the full range as defined by the patient scan conditions with a slice thickness corresponding to 3 mm and a voltage corresponding to 140 kV. The obtained CT images were transmitted via the radiation-therapy network system to the TPS to obtain target volumes and for organs at risk

[DOR: 20.1001.1.23223243.2021.19.1.4.5]

[DOI: 10.29252/ijrr.19.1.31]

(OAR) delineation. The regions of interest (ROIs) delineated in the ART phantom included the planning target volumes (PTV) and spinal cord, brainstem, parotid glands, tongue, larynx, external contour (skin), and Ring (Ring=skin–(skin–5mm)). Two skin-delineation methods were used, namely skin delineation with the immobilization device and skin delineation without the immobilization device. As shown in table 1, the relative electron density (RED) range for the entire ART phantom and ID (0.1–2.94) was within the range of the CT-ED calibration curve (0.1–3.74) in the TPS, thereby indicating that the TPS is capable of calculating the dose distribution in the ART and ID.

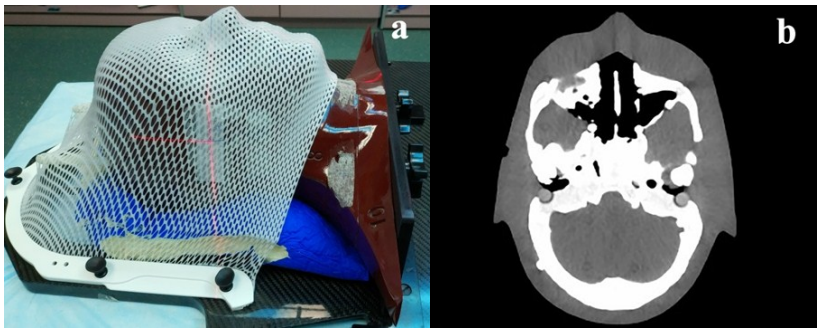

Figure 1. ART phantom and head-and-neck immobilization device used in simulation of the clinical-treatment process. **a)** Components of the immobilization device can be identified by their color: the thermoplastic mask is white, the Styrofoam bag is blue, and the carbon fiber base plate is black. **b)** Traverse section of the phantom slice.

Table 1. ART phantom HU and relative electron density from the CT images.

	HU			RED		
	Minimum	Mean	Maximum	Minimum	Mean	Maximum
ART phantom	-1023	-364	2976	0.1	0.64	2.94
Immobilization device	-1023	-841	419	0.1	0.22	1.28
TPS CT-ED calibration	-1023		4000	0.1		3.74

IMRT planning for patients and dose calculation

Ten patients under treatment for nasopharyngeal carcinomas with IMRT were selected retrospectively. All the patients were treated via the individualized head-and-neck immobilization device. The target volumes of the 10 patients, including the gross target volume of the nasopharynx (GTVnx), cervical lymph node (GTVnd), high-risk clinical target volume (CTV1), and low-risk clinical target volume (CTV2), were delineated by experienced oncologists based on ICRU Report Nos. 50 and 62 [19, 20]. The PTVs as obtained via a 3 mm uniform expansion from the CTVs were recorded as PTVnx, PTVnd, PTV1, and PTV2. The prescribed doses for PTVnx, PTVnd, PTV1, and PTV2 in the 30 fractions corresponded to 70 Gy, 64–66 Gy, 60 Gy, and 54 Gy, respectively. The IMRT plans used the dynamic multi-leaf collimator (dMLC) technique and consisted of nine equispaced coplanar beams. The dose was calculated via the X-ray Voxel Monte Carlo (XVMC) method with a maximum of 18 control points per beam, a calculation grid size of 3 mm × 3 mm × 3 mm, and a statistical uncertainty of 3% per control point.

For each patient, the treatment plan was transferred onto the ART phantom, and two QA plans were calculated. The QA plan with the immobilization device encompassed by the skin contour was denoted as “Plan-with” and that without the immobilization device was denoted as “Plan-without.” The differences between the doses calculated for the two cases were compared for each patient. Based on the dose volume parameters recommended in ICRU Report No. 83 [21], the assessment parameters selected for the PTVs were the near-maximum dose, $D_{2\%}$ (the dose received by 2% of the

[DOR: 20.1001.1.23223243.2021.19.1.4.5]
[DOI: 10.29252/ijrr.19.1.31]

volume of the ROIs), near-minimum dose, $D_{98\%}$ (the dose received by 98% of the volume of the ROIs), and mean dose received by the entire volume of the ROIs, D_{mean}. The assessment parameters for OARs were $D_{2\%}$ and D_{mean}.

Plan delivery

In this study, a Synergy accelerator with 6 MV X-rays was used with version 5.11 of the Monaco treatment planning system (TPS) (Elekta Ltd., Sweden) to provide radiation therapy. The machine was calibrated to deliver 1 cGy per monitor unit (MU) with a 10 cm square field at the depth at which the dose is a maximum for a source-to-surface distance of 100 cm. To simulate an actual patient treatment, the phantom was initially set up via lasers mounted on the wall. The IMRT plans of the patients were delivered to the ART phantom under conditions applied to the patient's actual radiation exposure (actual angles, considering the immobilization device).

EBT3 film calibration and dose measurements

The EBT3 film is symmetrical and sandwich-shaped. It contains an intermediate 28-μm active slice and upper and lower 125-μm polyester protective sheets. EBT3 films can be used to effectively measure doses ranging from 0.01 to 30 Gy, thereby satisfying the requirements of the study [22]. A single-film calibration method was used to obtain the film calibration dose curve as shown in figure 2b for fast dose calibration. The EBT3 films used in the study were all obtained from the same batch (No. 11091602) with the dose of the film correction curve ranging from 0–4 Gy. Radiation was applied in 10 static step fields (5 cm × 10 cm) on two different films (figure 2a). A PTW UNIDOSE dosimeter and a PTW30013 0.6-cc ionization chamber were used for absolute dose measurements, and a dose measurement was performed for all the steps to ensure that the effect of the scattered dose was considered. An EPSON 10000XL flatbed scanner was used in 48-bit RGB mode to scan films at a resolution of 72 dpi. During the scanning process, the center of the films and scanner were coaxially aligned, and the long sides of all the films were parallel to the scanning direction. The scan results were imported into commercial film-dose analysis software (QAchart, V2.1, Raydose Inc., Guangzhou) via the triple-channel analysis method [23, 24].

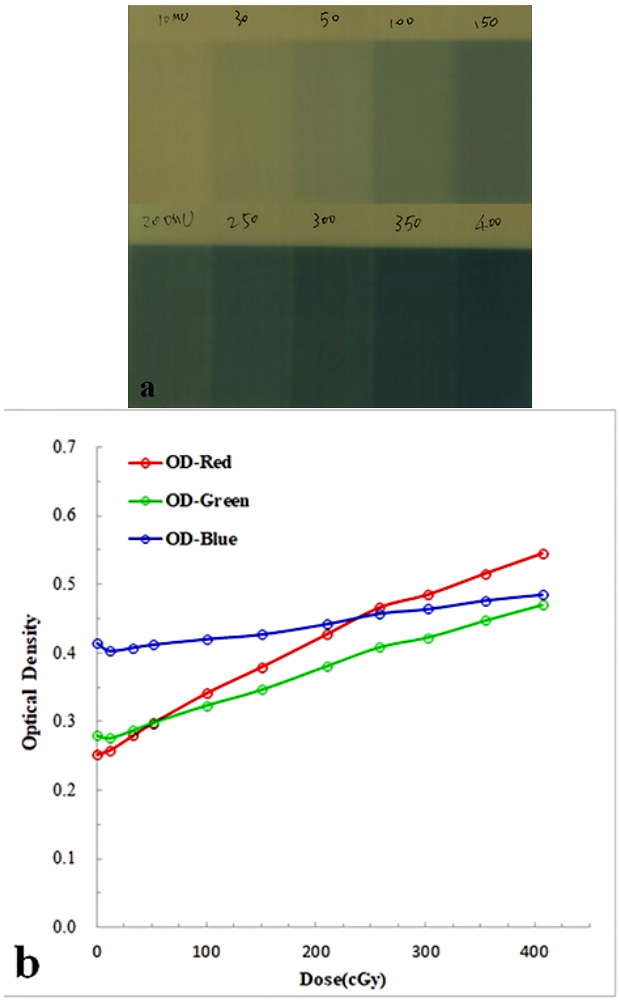

Figure 2. EBT3 dosimetry film and dose calibration curves. **a)** EBT3 film after step-wise irradiation. **b)** EBT3 dose calibration curves for triple-channel analysis.

The films used for the measurements were cut into 7.8 cm × 14.5 cm strips and sandwiched between the fifth and sixth transverse sections of the phantom. A specific point on the posterior of the neck was selected and marked as a reference to compare the TPS-calculated doses. In addition to comparing the doses estimated for 10 patients using the Plan-with and Plan-without configurations, we also compared the doses with actual film measurements. The difference between the doses measured with the films and

doses calculated by QA plans were analyzed. The gamma-passing rates for global maximum dose normalization in absolute dose were calculated and compared by using different dose-deviation and distance-deviation criteria (i.e., 5%/3 mm, 3%/3 mm, 3%/2 mm, and 2%/2 mm).

Statistical analysis

Data were expressed as mean ± standard deviation (SD) and analyzed via SPSS version 23.0 software (IBM Inc., USA). A Wilcoxon signed rank test was performed to evaluate the existence of a significant difference between Plan-with and Plan-without in gamma passing rates and dose parameters for PTVs and OARs. Additionally, p values <0.05 were considered as statistically significant.

RESULTS

Dose validation by EBT3 film measurement

Figure 3 shows the results of film measurement verification for a certain patient. The dose distribution profile indicated that the dose measured during treatment delivery was relatively close to the dose distribution of Plan-with. The results of measurement verification for all patients are summarized in table 2. As shown in the table, based on absolute dose comparisons, the global gamma passing rate for Plan-with exceeded the rate for Plan-without under different calculation criteria. With the commonly used 3%/3 mm criterion, the gamma passing rate corresponded to 92.0 ± 2.1% for Plan-with and only 82.8 ± 6.9% for Plan -without. Hence, the dose measured in the ART phantom was closer to the dose calculated by the TPS when the immobilization device is considered.

The dose measured in the skin at the posterior of the neck was closer to the value calculated using Plan-with that considered the immobilization device with a mean deviation of 1.8% (-6.5% to 15.7%) being observed. Conversely, EBT3 film measurements differed significantly from the values calculated using Plan-without, which did not consider the immobilization device. A mean deviation of -33.1% (-19.3 to -52.4%) was observed as shown in figure 4. Hence, the radiation dose in the patient's skin was significantly underestimated using Plan-without.

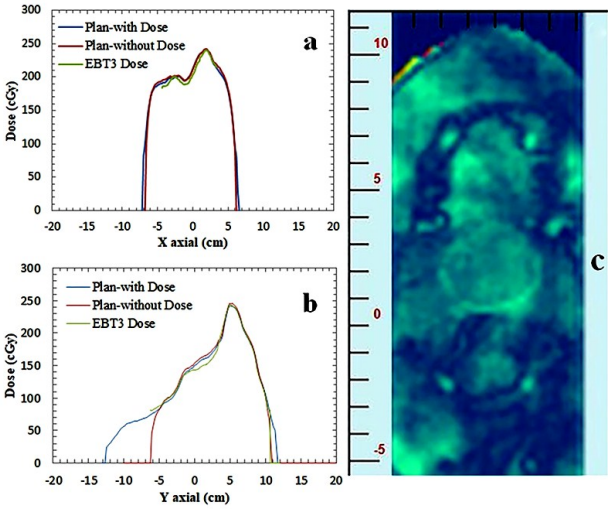

Figure 3. Absolute comparison of doses measured using EBT3 films with TPS-calculated doses. **a)** X-axis profile. **b)** Y-axis profile. **c)** gamma-value distribution for Plan-with under the 3%/3 mm criterion.

Table 2. Gamma passing rates (%) of the ten NPC IMRT plans as validated by ART phantoms and EBT3 film measurements.

	5%/3 mm	3%/3 mm	3%/2 mm	2%/2 mm
Plan-without	95.78 ± 2.43	82.76 ± 6.90	75.44 ± 7.86	62.67 ± 10.85
Plan-with	98.24 ± 1.33	92.03 ± 2.06	86.71 ± 2.40	75.49 ± 2.43
p	0.037	0.005	0.005	0.007

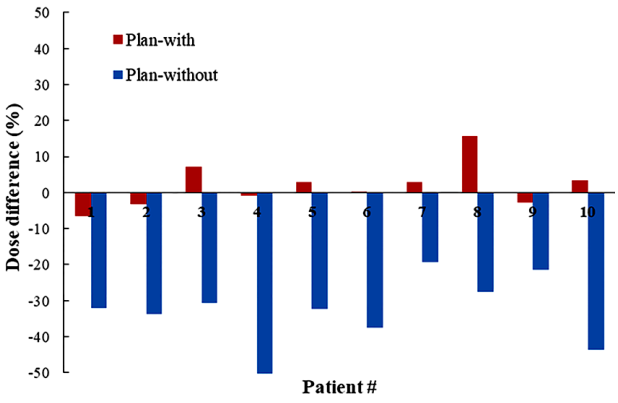

Figure 4. Dose difference between TPS-calculated and EBT3 film-measured doses on the skin at the posterior of the neck.

[DOR: 20.1001.1.23223243.2021.19.1.4.5]
[DOI: 10.29252/ijrr.19.1.31]

Impact of immobilization device on dose of PTVs and OARs

For each target volume, $D_{2\%}$, $D_{98\%}$, and D_{mean} in Plan-with were 1–4% lower than those in Plan-without. Additionally, a significant dose reduction was observed in the lymph node target volume (PTVnd). Furthermore, a 1–3% reduction was observed in the value of $D_{2\%}$ and D_{mean} for normal tissue as summarized in table 3.

Table 3. Dose parameters (Gy) for PTVs and OARs in 10 NPC patients as calculated by the two ART phantom plans.

ROIs	Parameters	Plan-with	Plan-without	Plan-with/ Plan-without	*P*
PTVnx	$D_{2\%}$	76.31± 4.34	77.45± 1.39	0.98 ± 0.33	0.005
	$D_{98\%}$	56.18± 4.72	57.40± 4.72	0.98 ± 0.32	0.005
	D_{mean}	69.48± 1.62	70.56± 1.65	0.98 ± 0.33	0.005
PTVnd	$D_{2\%}$	68.98± 2.85	71.90± 3.30	0.96 ± 0.29	0.005
	$D_{98\%}$	50.20± 3.95	51.40± 4.05	0.98 ± 0.32	0.005
	D_{mean}	60.68± 4.13	62.54± 4.28	0.97 ± 0.32	0.005
PTV1	$D_{2\%}$	71.12± 1.22	72.19± 1.24	0.98 ± 0.33	0.005
	$D_{98\%}$	47.41± 4.25	48.59± 4.42	0.98 ± 0.32	0.005
	D_{mean}	62.12± 1.88	63.24± 1.93	0.98 ± 0.33	0.005
PTV2	$D_{2\%}$	69.84± 1.22	70.92± 1.24	0.98 ± 0.33	0.005
	$D_{98\%}$	33.71± 7.44	33.99± 7.61	0.99 ± 0.33	0.021
	D_{mean}	55.08± 6.61	56.08± 2.83	0.98 ± 0.33	0.005
PRV-BrainStem	$D_{2\%}$	52.84± 6.11	53.56± 6.02	0.99 ± 0.33	0.005
	D_{mean}	32.79± 4.40	33.16± 4.41	0.99 ± 0.33	0.005
PRV-Spinal	$D_{2\%}$	40.99± 2.40	42.45± 2.48	0.97 ± 0.32	0.005
	D_{mean}	30.08± 4.09	31.85± 4.21	0.97 ± 0.32	0.005
Parotid	$D_{2\%}$	63.22± 3.29	64.99± 3.36	0.97 ± 0.32	0.005
	D_{mean}	46.55± 3.70	46.67± 3.67	0.99 ± 0.33	0.052
Tongue	$D_{2\%}$	56.33± 3.38	57.25± 3.43	0.98 ± 0.33	0.005
	D_{mean}	41.83± 5.43	42.37± 5.52	0.99 ± 0.33	0.005
Larynx	$D_{2\%}$	55.61± 3.92	57.48± 4.18	0.97 ± 0.32	0.005
	D_{mean}	43.13± 3.02	44.27± 3.32	0.97 ± 0.33	0.005
Ring	$D_{2\%}$	52.42± 4.11	49.28± 3.88	1.03±0.01	0.005
	D_{mean}	19.98± 2.43	17.42± 2.10	1.10±0.02	0.005

Effect of immobilization device on volume distribution

The three-dimensional distribution of the difference in the dose shown in figure 5 was obtained by direct subtraction of the two QA plans of a certain patient's treatment plan (Plan-with – Plan-without). This image was used to assess the effect of the immobilization device on the treatment plan where the blue-to-red gradients represented absolute differences in dose ranging from -6–30 Gy. The end-to-end test indicated that a significant difference was observed in the dose distribution due to the attenuation and bolus effect of the immobilization device. The dose in the body was slightly decreased, due to attenuation, while the radiation scattering and build-up effect caused by the Styrofoam bag between the posterior of the patient's neck and carbon fiber base plate increased the dose in the skin by approximately 3.1 Gy.

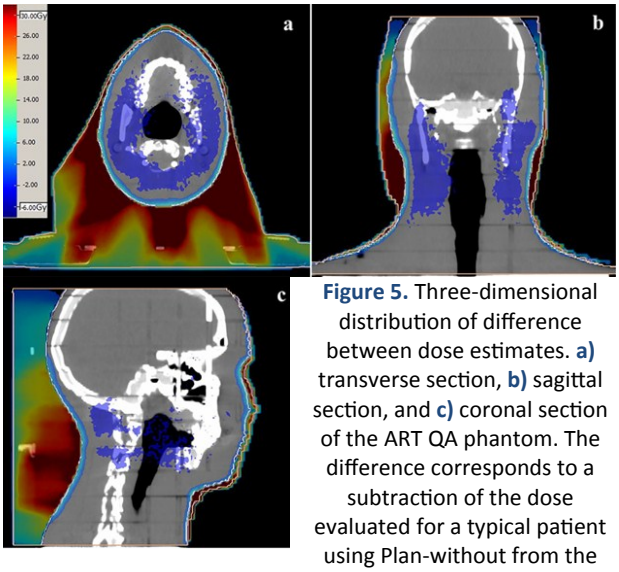

Figure 5. Three-dimensional distribution of difference between dose estimates. **a)** transverse section, **b)** sagittal section, and **c)** coronal section of the ART QA phantom. The difference corresponds to a subtraction of the dose evaluated for a typical patient using Plan-without from the dose evaluated using Plan-with.

DISCUSSION

In the present study, an end-to-end test using the ART phantom and EBT3 film was performed to assess the overall accuracy of dose delivery. The current dose verification equipment including ionization chambers, ion chamber or diode arrays, and three-dimensional verification

equipment exhibits different shapes and densities from those of actual patients. Additionally, it is not possible to verify the effect of the immobilization device on the plan delivery with measurements performed by the aforementioned equipment. The ART phantom used to simulate the anatomy of a patient in the study contained tissue-equivalent material that makes it closer to an actual human than a solid water phantom in appearance and internal structure. EBT3 film material is near-tissue-equivalent (effective atomic number 6.84), and the film exhibits a high spatial resolution with a response that is independent of the high energy and angle [25-27]. Therefore, it is more suitable to measure the dose distribution from an end-to-end test by using an ART phantom.

The effect of the patient's immobilization device on the implementation of the treatment plan was overlooked during treatment planning for nasopharyngeal carcinomas. Studies indicated that the treatment table and immobilization device can produce attenuation and bolus effects on radiation, thereby reducing the actual dose received by the target volume and increasing the dose absorbed by the skin [28-30]. A study by Seppälä et al. indicated that the attenuation of the 6-MV rays by the treatment table varied with the angle of incidence (90–180°) by up to 8%. Butson et al. used dosimetry films and measured a 37–66% increase in the skin dose when the beam was inclined on the carbon-fiber base plate [5]. A study by Lee *et al.* indicated that in the treatment of prostate cancer, skin dose values measured at the inguinal region with a thermoluminescent dosimeter (TLD) were closer to the doses for skin delineation calculated by the TPS when a carbon-fiber base plate and vacuum bag devices were included [4]. Therefore, the effects of the accessories on radiation attenuation and skin dose should be considered in a comprehensive manner when a radiation beam travels through a treatment table or an immobilization device.

Currently, a virtual model of the treatment table (including geometric and density information) is typically included in a TPS to calculate the attenuating effect of this treatment table on the treatment plan [31]. In the present study, the immobilization device was modeled in the TPS as encompassed by the skin contour to calculate the effect of it on the dose distribution in IMRT for NPC. Given the dose-attenuating effect of the immobilization device, the values of $D_{2\%}$, $D_{98\%}$, and D_{mean} for the target volume dose as calculated for Plan-with decreased by 1–4% when compared to those calculated for Plan-without. This is consistent with the results of the study by Arthur et al., which indicated that immobilization devices composed entirely of carbon-fiber materials exhibited a 2–4% attenuating effect on incident radiation [32]. The dose reduction for PTVnd was most pronounced with a reduction of 4% for the maximum and 3% for the mean dose (table 3). This is mainly due to decreases in distance between PTVnd and the immobilization device and more pronounced attenuation that occurs when radiation penetrates the immobilization device. The values of $D_{2\%}$ and D_{mean} for the OARs also tended to decrease, and a maximum reduction of 3% was observed. Thus, TPS calculations indicated that the dose within the delineated ROIs decreased when the immobilization device was considered due to attenuation effects.

Table 2 lists the gamma passing rate of 10 NPC intensity-modulated radiation therapy plans by considering the actual beam angle, as validated with the ART phantom and EBT3 film measurements. The verification results for Plan-with exceeded those for Plan-without. Furthermore, the film dose distribution profile as measured during treatment delivery was relatively close to the dose distribution of Plan-with (figure 3). This indicated that the doses calculated by TPS without considering the immobilization device in the body contour were not consistent with the actual clinically delivered dose. With respect to skin doses at posterior of the patient's neck, the results obtained with Plan-with were close to the doses measured with EBT3 film (mean deviation of 1.3%) while those obtained with Plan-without underestimated the doses by approximately 33.1% (figure 4). This significantly exceeded the results obtained by Lee et al., which displayed an average increase in the skin dose of patients of

[DOR: 20.1001.1.23223243.2021.19.1.4.5]
[DOI: 10.29252/ijrr.19.1.31]

18% in the presence of a thermoplastic mask using an anthropomorphic phantom and TLDs [33]. The TPS calculation suggested that the dose to the skin increased by 3.1 Gy due to the bolus effect of the low-density polystyrene foam material between the neck and carbon-fiber base plate and the thermoplastic mask. Hoppe et al. reported that, in stereotactic body radiation therapy planning for treatment of early non-small cell lung cancer, the skin dose of patients increased because the presence of accessories (the treatment table and vacuum bag) was ignored, and 38% of patients experienced acute skin radiation toxicity while a patient experienced Grade 4 skin toxicity [34]. Hence, we recommend that the head-and-neck immobilization device should be delineated into the body contour during treatment planning by considering the increased skin dose caused by the immobilization device, such that the TPS dose calculation is more in line with the actual clinically delivered dose.

In conclusion, the application of an end-to-end test using the anthropomorphic phantom indicated that head-and-neck immobilization devices decrease radiation doses in PTVs and OARs in IMRT for nasopharyngeal carcinoma due to the attenuation effect and increase skin dose in the neck's posterior due to the bolus effect. As a result, the body contour should include the immobilization device to ensure consistency between the delivery dose and planning dose. Hence, the end-to-end test is very useful to identify discrepancies between the calculated and delivered doses during radiation therapy, and it can serve as a valuable tool for patient-specific QA.

ACKNOWLEDGEMENT

This work was supported by the Anhui Provincial Natural Science Foundation (No. 1808085QA13 and 1708085QC80).

***Conflicts of interest*: Declared none.**

REFERENCES

1. Pan XB, Huang ST, Chen KH, Jiang YM, Ma JL, Qu S, Li L, Chen L, Zhu XD (2017) Intensity-modulated radiotherapy provides better quality of life than two-dimensional conventional radiotherapy for patients with stage II nasopharyngeal carcinoma. *Oncotarget,* ***8(28)****: 46211-8*.
2. Qiu WZ, Peng XS, Xia HQ, Huang PY, Guo X, Cao KJ (2017) A retrospective study comparing the outcomes and toxicities of intensity-modulated radiotherapy versus two-dimensional conventional radiotherapy for the treatment of children and adolescent nasopharyngeal carcinoma. *J Cancer Res Clin,* ***143(8)****: 1563-72*.
3. Wang WD, Feng M, Fan ZX, Li J, Lang JY (2014) Clinical outcomes and prognostic factors of 695 nasopharyngeal carcinoma patients treated with intensity-modulated radiotherapy. *Biomed Res Int, 2014: 814948(1-10).*
4. Lee KW, Wu JK, Jeng SC, Liu YWH, Cheng JCH (2009) Skin dose impact from vacuum immobilization device and carbon fiber couch in intensity modulated radiation therapy for prostate cancer. *Med Dosim,* ***34(3)****: 228-32*.
5. Butson MJ, Cheung T, Yu PKN (2007) Megavoltage X-ray skin dose variation with an angle using grid carbon fibre couch tops. *Phys Med Biol,* ***52(20)****: N485-N92*.
6. Olch AJ, Gerig L, Li H, Mihaylov I, Morgan A (2014) Dosimetric effects caused by couch tops and immobilization devices: Report of AAPM Task Group 176. *Med Phys,* ***41 (6)****: 061501(1-30).*
7. Miften M, Olch A, Mihailidis D, Moran J, Pawlicki T, Molineu A, Li H, Wijesooriya K, Shi J, Xia P, Papanikolaou N, Low DA (2018) Tolerance limits and methodologies for IMRT measurement-based verification QA: Recommendations of AAPM Task Group No. 218. *Med Phys,* ***45(4)****: E53-E83*.
8. Saenz DL, Narayanasamy G, Cruz W, Papanikolaou N, Stathakis S (2016) Pinnacle(3) modeling and end-to-end dosimetric testing of a Versa HD linear accelerator with the Agility head and flattening filter-free modes. *J Appl Clin Med Phys,* ***17(1)****: 192-206*.
9. Kutcher GJ, Coia L, Gillin M, Hanson WF, Leibel S, Morton RJ, Palta JR, Purdy JA, Reinstein LE, Svensson GK, Weller M, Wingfield L (1994) Comprehensive Qa for Radiation Oncology - Report of Aapm Radiation-Therapy Committee Task-Group-40. *Med Phys,* ***21(4)****: 581-618*.
10. Klein EE, Hanley J, Bayouth J, Yin FF, Simon W, Dresser S, Serago C, Aguirre F, Ma LJ, Arjomandy B, Liu C, Sandin C, Holmes T (2009) Task Group 142 report: Quality assurance of medical accelerators. *Med Phys,* ***36(9)****: 4197-212*.
11. Fraass B, Doppke K, Hunt M, Kutcher G, Starkschall G, Stern R, Van Dyke J (1998) American Association of Physicists in Medicine radiation therapy committee task group 53: Quality assurance for clinical radiotherapy treatment planning. *Med Phys,* ***25(10)****: 1773-829*.

12. Wesolowska P, Georg D, Lechner W, Kazantsev P, Bokulic T, Tedgren AC, Adolfsson E, Campos AM, Leandro Alves VG, *et.al*. (2019) Testing the methodology for a dosimetric end-to-end audit of IMRT/VMAT: results of IAEA multicentre and national studies. *Acta Oncologica,* ***58(12)****: 1731-9*.
13. Tuntipumiamorn L, Tangboonduangjit P, Sanghangthum T, Rangseevijitprapa R, Khamfongkhruea C, Niyomthai T, *et.al*. (2019) Multi-institutional evaluation using the end-to-end test for implementation of dynamic techniques of radiation therapy in Thailand. Reports of practical oncology and radiotherapy. *journal of Greatpoland Cancer Center in Poznan and Polish Society of Radiation Oncology,* ***24 (1)****: 124-32*.
14. Calusi S, Noferini L, Marrazzo L, Casati M, Arilli C, Compagnucci A, Talamonti C, Scoccianti S, Greto D, Bordi L, Livi L, Pallotta S (2017) gamma Tools: A modular multifunction phantom for quality assurance in GammaKnife treatments. *Phys Medica,* ***43****: 34-42*.
15. Kumazaki Y, Ozawa S, Nakamura M, Kito S, Minemura T, Tachibana H, Nishio T, Ishikura S, Nishimura Y (2018) An end-to-end postal audit test to examine the coincidence between the imaging isocenter and treatment beam isocenter of the IGRT linac system for Japan Clinical Oncology Group (JCOG) clinical trials. *Phys Medica,* ***53****: 145-52*.
16. Poder J, Brown R, Porter H, Gupta R, Ralston A (2018) Development of a dedicated phantom for multi-target single-isocentre stereotactic radiosurgery end to end testing. *J Appl Clin Med Phys,* ***19(6)****: 99-108*.
17. Kazantsev P, Lechner W, Gershkevitsh E, Clark CH, Venencia D, Van Dyk J, Wesolowska P, Hernandez V, *et al.* (2019) IAEA methodology for on-site end-to-end IMRT/VMAT audits: an international pilot study. *Acta Oncologica,* ***59(2)****: 141-148*.
18. Loughery B, Knill C, Silverstein E, Zakjevskii V, Masi K, Covington E, Snyder K, Song K, Snyder M (2019) Multi-institutional evaluation of end-to-end protocol for IMRT/VMAT treatment chains utilizing conventional linacs. *Med Dosim,* ***44(1)****: 61-6*.
19. Landberg T, Chavaudra J, Dobbs J, Landberg T, Chavaudra J, Dobbs J, Dobbs J (1993) Prescribing, recording and reporting photon beam therapy: ICRU Report 50. Journal of the International Commission on Radiation Units and Measurements, os26:NP. doi.org/10.1093/jicru/os26.1.
20. Landberg T, Chavaudra J, Dobbs J, Landberg T, Chavaudra J, Dobbs J, Dobbs J (1999) Prescribing, recording and reporting photon beam therapy (Supplement to ICRU Report 50): ICRU Report 62. Journal of the International Commission on Radiation Units and Measurements, os32:NP. doi.org/10.1093/jicru/os32.1.
21. Grégoire V, Mackie TR, De Neve W, Gospodarowicz M, Purdy JA, van Herk M, Niemierko A, (2010) Prescribing, recording, and reporting photon-beam intensity-modulated radiation therapy (IMRT): ICRU Report 83. *Journal of the International Commission on Radiation Units and Measurements,* ***10(1)****: 1-106*.
22. Devic S, Tomic N, Lewis D (2016) Reference radiochromic film dosimetry: Review of technical aspects. *Phys Medica,* ***32(4)****: 541-56*.
23. Azorin JFP, Garcia LIR, Marti-Climent JM (2014) A method for multichannel dosimetry with EBT3 radiochromic films. *Med Phys,* ***41(6)****: 062101.*
24. Paelinck L, De Neve W, DeWagter C (2007) Precautions and strategies in using a commercial flatbed scanner for radiochromic film dosimetry. *Phys Med Biol,* ***52(1)****: 231-42*.
25. Borca VC, Pasquino M, Russo G, Grosso P, Cante D, Sciacero P, Girelli G, La Porta MR, Tofani S (2013) Dosimetric characterization and use of Gafchromic EBT3 film for IMRT dose verification. *J Appl Clin Med Phys,* ***14(2)****: 158-71*.
26. Fuss M, Sturtewagen E, De Wagter C, Georg D (2007) Dosimetric characterization of Gafchromic EBT film and its implication on film dosimetry quality assurance. *Phys Med Biol,* ***52(14)****: 4211-25*.
27. Arjomandy B, Tailor R, Anand A, Sahoo N, Gillin M, Prado K, Vicic M (2010) Energy dependence and dose response of Gafchromic EBT2 film over a wide range of photon, electron, and proton beam energies. *Med Phys,* ***37(5)****: 1942-7*.
28. Li H, Lee AK, Johnson JL, Zhu RX, Kudchadker RJ (2011) Characterization of dose impact on IMRT and VMAT from couch attenuation for two Varian couches. *J Appl Clin Med Phys,* ***12(3)****: 23-31*.
29. Kry SF, Smith SA, Weathers R, Stovall M (2012) Skin dose during radiotherapy: a summary and general estimation technique. *J Appl Clin Med Phys,* ***13(3)****: 20-34*.
30. Seppala JKH and Kulmala JAJ (2011) Increased beam attenuation and surface dose by different couch inserts of treatment tables used in megavoltage radiotherapy. *J Appl Clin Med Phys,* ***12(4)****: 15-23*.
31. Gerig LH, Niedbala M, Nyiri BJ (2010) Dose perturbations by two carbon fiber treatment couches and the ability of a commercial treatment planning system to predict these effects. *Med Phys,* ***37(1)****: 322-8*.
32. Olch AJ and Lavey RS (2002) Reproducibility and treatment planning advantages of a carbon fiber relocatable head fixation system. *Radiother Oncol,* ***65(3)****: 165-8*.
33. Lee N, Chuang C, Quivey JM, Phillips TL, Akazawa P, Verhey LJ, Xia P (2002) Skin toxicity due to intensity-modulated radiotherapy for head-and-neck carcinoma. *Int J Radiat Oncol,* ***53(3)****: 630-7*.
34. Hoppe BS, Laser B, Kowalski AV, Fontenla SC, Pena-Greenberg E, Yorke ED, Lovelock DM, Hunt MA, Rosenzweig KE (2008) Acute skin toxicity following stereotactic body radiation therapy for stage I non-small-cell lung cancer: Who's at risk? *Int J Radiat Oncol,* ***72(5)****: 1283-6*.